

IMAGE SEGMENTATION AND REGISTRATION ALGORITHM TO COLLECT HOMOLOGOUS LANDMARKS FOR AGE-RELATED THORACIC MORPHOMETRIC ANALYSIS

Ashley A. Weaver
Elizabeth G. Armstrong
Elizabeth A. Moody
Joel D. Stitzel

Virginia Tech – Wake Forest University Center for Injury Biomechanics
Wake Forest University School of Medicine
Medical Center Boulevard, Winston Salem, NC, 27157
USA
Paper Number 11-0317

ABSTRACT

Skeletal and physiological resilience are known to decline with age, resulting in a decreased ability for the body to withstand traumatic insults. Adults 65 years of age and older currently constitute more than 12% of the total population and the elderly population is projected to reach nearly 20% by 2030. The objective of the current study is to quantify age and gender-specific variations in the thoracic skeletal morphology for use in generating a parametric thoracic model for injury prediction. This goal will be accomplished using the image segmentation and registration algorithm developed in this study to collect homologous (or comparable) landmarks from the ribs. A minimum of 10 normal chest CT scans for each gender were collected from a radiological database for the following age groups: newborns, 3 month, 6 month, 9 month, 1 year, 3 year, and 6 year olds. Beginning with 10 year olds, a minimum of 10 CT scans for each gender were collected by decade up to age 100. Image segmentation and subsequent image registration of the collected scans was used to collect homologous rib landmarks. A semi-automated method was used to segment each rib and create a mask and three-dimensional (3D) model. Thresholding and region growing operations were applied and manual editing was used to ensure selection of the entire rib and exclusion of surrounding soft tissue. An atlas was created from segmentation of a normal chest CT scan of an average male with over 1,000 landmark points placed on each rib. Each segmented rib is registered to the atlas. Rigid, affine, and non-rigid, nonlinear transformations are used to morph the atlas to the subject rib. The transformation matrices are used to map the landmarks in the atlas coordinate system to the subject-specific coordinate system. Effectively, this allows for collection of homologous rib landmarks across subjects of all ages. Geometric morphometrics, particularly the Procrustes superimposition method can then be used to analyze the landmark data to formulate age and gender-

specific shape and size variation functions. Shape and size functions computed from the landmark data can be used to create a scalable finite element model of the thorax that will allow vehicle crashworthiness to be evaluated for all ages and genders and will lead to improvements in restraint systems to better protect children and elderly in a crash.

INTRODUCTION

In motor vehicle crashes, thoracic injury ranks second only to head injury in terms of the number of fatalities and serious injuries, the body region most often injured, and the overall economic cost (Cavanaugh 2002; Ruan, El-Jawahri et al. 2003). Thoracic injuries account for 13% of all minor to moderate injuries, 29% of all serious to fatal injuries, and are attributed to up to 25% of traumatic deaths (Dougall, Paul et al. 1977; Galan, Penalver et al. 1992; Allen and Coates 1996; Ruan, El-Jawahri et al. 2003). While motor vehicle crashes are associated with 60-70% of blunt chest trauma, 20% is attributed to falls that are more commonly seen in the elderly (Galan, Penalver et al. 1992; Allen and Coates 1996).

Adults 65 years of age and older currently constitute more than 12% of the total population and with increases in life expectancy, the elderly population is projected to reach nearly 20% by 2030 (U.S. Census Bureau 2008). Motor vehicle crash is a common source of trauma among the elderly population, with the elderly having the second highest crash-related death rate compared to all age groups (National Center for Health Statistics 2003). The incidence of thoracic injury increases with age for both belted and unbelted occupants (Hanna 2009). Skeletal and physiological resilience are known to decline with age, resulting in a decreased ability for the body to withstand traumatic insults (Burststein, Reilly et al. 1976; Zioupos and Currey 1998). Thoracic injury tolerance in the elderly has been shown to decrease by 20% for blunt loading and up to 70% for concentrated belt-loading (Zhou 1996).

Thoracic morbidity and mortality also increase with age. Older patients sustaining a thoracic injury present with more comorbidities, develop more complications, remain on a ventilator longer, and require longer stays in the intensive care unit and hospital (Finelli, Jonsson et al. 1989; Shorr, Rodriguez et al. 1989; Perdue, Watts et al. 1998; Holcomb, McMullin et al. 2003; Hanna 2009). Complications from thoracic injury include pneumonia, atelectasis, acute respiratory distress syndrome, and respiratory failure. Elderly patients with rib fractures have two to five times the risk of mortality of younger patients with increases in risk observed as the number of rib fractures increase (Bergeron, Lavoie et al. 2003; Stawicki, Grossman et al. 2004). Each additional rib fracture results in a 19% increase in mortality and 27% increase in pneumonia (Bulger, Arneson et al. 2000). A recent study used a receiver-operator characteristic analysis to identify the age thresholds associated with increased mortality in 12 leading thoracic injuries (Stitzel, Kilgo et al. 2010). Although many thresholds were near the traditional age threshold of 55 years commonly used to identify patients of increased mortality risk, the study found age thresholds that were injury-specific. For instance, the age threshold for bilateral pulmonary contusion indicates patients older than 46 years with this injury have an increased mortality risk compared to patients younger than 46.

Age and gender-specific variations in the geometry and mechanics of the thoracic skeleton are expected to relate to thoracic injury. Previous studies have found statistically significant changes in the rib cage geometry with age (Kent, Lee et al. 2005; Gayzik, Yu et al. 2008). However, these studies had several limitations. Geometrical changes such as the shape, size, and angle of the ribs were quantified using a limited number of landmarks or measurements that were collected manually from two-dimensional (2D) images of a computed tomography (CT) scan. Also, the pediatric population was not analyzed in either of these studies and some other age groups were under-represented. The objective of the current study is to quantify age and gender-specific variations in the thoracic skeletal morphology for both genders and across the entire age spectrum (ages 0-100). This goal will be accomplished using a semi-automated image segmentation and registration algorithm to collect homologous landmarks from the ribs.

METHODS

An algorithm was developed to collect landmark data from the ribs for the purpose of quantifying age and gender-specific variations. The main steps of the

algorithm are: 1) Scan Collection, 2) Image Segmentation, and 3) Image Registration.

Scan Collection

Normal chest CT scans of males and females ages 0-100 were collected from the radiological database at Wake Forest University Baptist Medical Center. To identify exclusion criteria and ensure normal scans were collected, a musculoskeletal radiologist was consulted. Exclusion criteria included, but were not limited to: congenital abnormalities, infections, fractures, and cancers of the ribs, scoliosis, kyphosis, sternotomy, thoracotomy, and osteopenia or osteoporosis in individuals younger than 50. Radiology reports and other patient medical records were reviewed and scans were visually inspected. A minimum of 10 male and 10 female scans were collected for the following age groups: newborns, 3, 6, and 9 month, 1, 3, and 6 year olds. Beginning with 10 year olds, 10 scans for each gender were collected by decade up to age 100 (Figure 1, Figure 2).

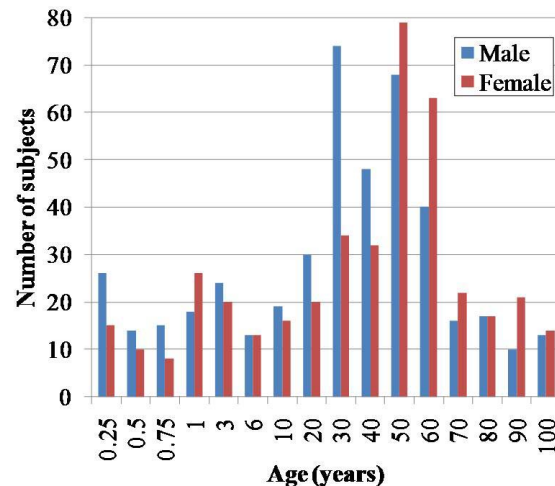


Figure 1. Histogram of CT scans collected with age values representing the upper bin limit.

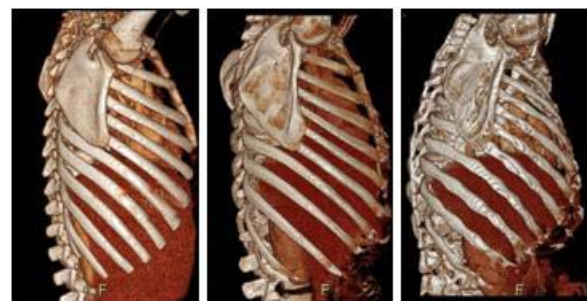


Figure 2. 3D CT reconstructions (left to right): 6, 29, and 73 year old subjects. Morphological thoracic skeletal differences of the pediatric, young adult, and elderly subjects are evident.

Image Segmentation

A semi-automated method was used to segment the 24 ribs on each subject. A bone threshold was applied, followed by a region growing operation. Minimal manual editing was used to ensure the entire rib was selected and the surrounding soft tissue was excluded. Calcified costal cartilage was excluded when present. A hole filling operation was used to enclose the rib interior. Each rib cage segmentation takes one to five hours depending on the subject size, bone density, and other factors. Results of the segmentation include a mask and a three-dimensional (3D) model for each rib (Figure 3).

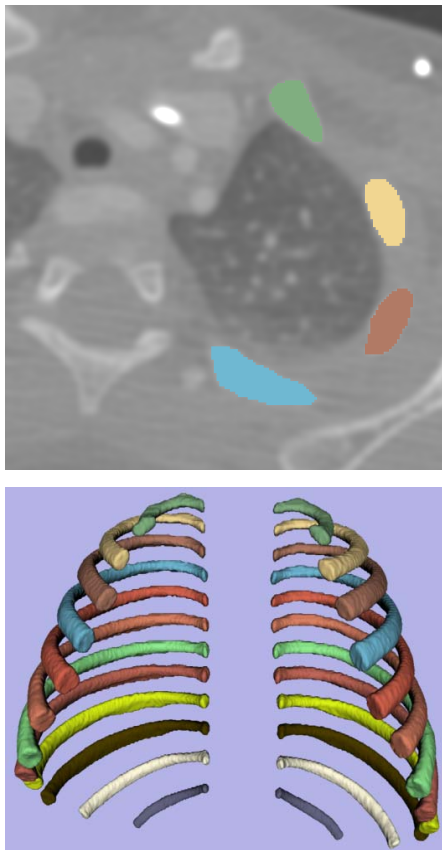


Figure 3. Rib segmentation results. Top photo: Masks of the segmented left ribs 1-4 overlaid on an axial chest CT image. Bottom photo: 3D models of the 24 segmented ribs of a pediatric subject.

Image Registration

An image registration algorithm was developed for the purpose of collecting homologous landmarks from the ribs for all subjects in the study. The image registration algorithm requires minimal user interaction and takes approximately five to ten

minutes per rib. An atlas was created from segmentation of a normal chest CT scan of an average male. The atlas contained the 24 ribs with over 1,000 landmark points placed on each rib as illustrated in Figure 4. For every subject in the study, each segmented rib was registered with the corresponding rib in the atlas (i.e. the left first rib in each subject is registered with the left first rib in the atlas). Rigid, affine, and non-rigid, non-linear transformations were used in the registration algorithm to morph the atlas and its landmarks to the rib of each subject (Figure 5, Steps 1 and 2). Following the registration, the 1,000+ landmark points on each rib have been transformed to the subject-specific coordinate system of the CT scan (Figure 5, Step 3). Effectively, this allows for collection of homologous rib landmarks across subjects of all ages.



Figure 4. Right third rib from the atlas with 1,000 landmarks placed.

RESULTS

An example of the results of the registration algorithm is provided in Figure 6. In this example the left fourth rib from a 16 year old male (termed “subject rib”) was registered with the left fourth rib of the average male (termed “atlas rib”). The rigid transformation (Figure 6, Step 1) translates and rotates the atlas rib to align three landmarks on the atlas rib with three landmarks on the subject rib. The affine transformation (Figure 6, Step 2) applies

translation, rotation, scaling, and shearing operations to morph the atlas rib to the subject rib. In the final step of the registration algorithm, a non-rigid, non-

linear transformation is applied to morph the atlas rib to the subject rib (Figure 6, Step 3).

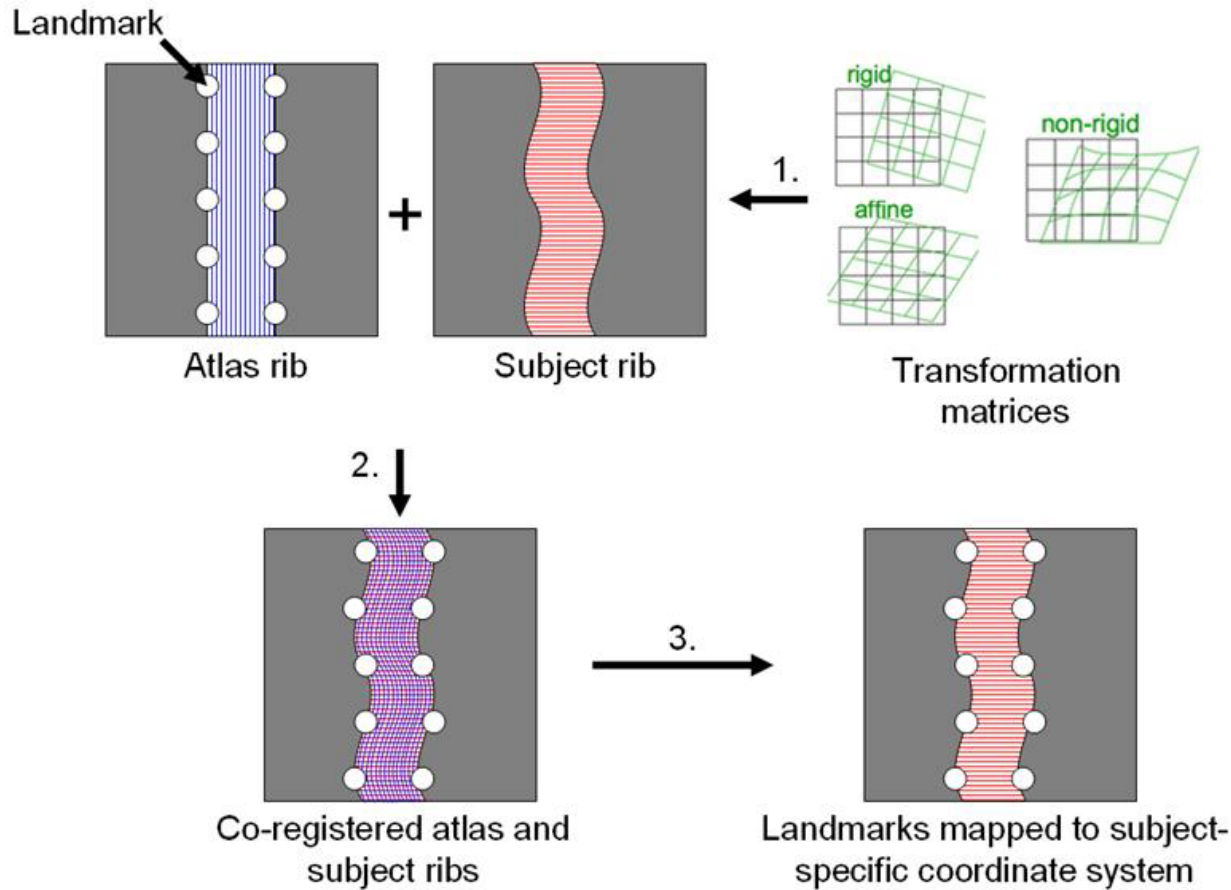


Figure 5. Image registration process. 1) Rigid, affine, and non-rigid, non-linear transformations are applied to register a subject's rib with the atlas. The atlas rib is depicted with only 10 landmarks for simplification. 2) The co-registered atlas rib and subject rib in the subject-specific coordinate system with 10 landmarks shown. 3) Depiction of 10 landmarks mapped to the subject-specific coordinate system.

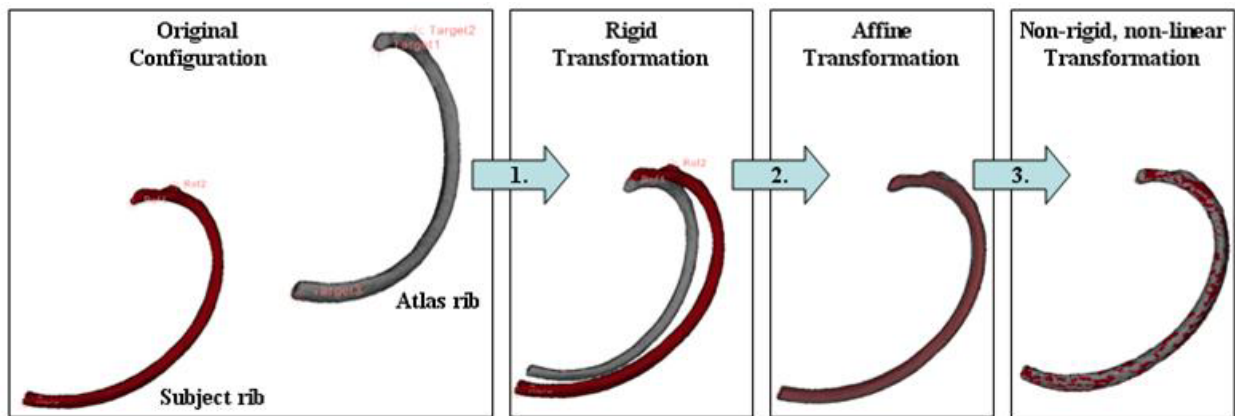


Figure 6. Image registration example. 1) Rigid transformation is applied to rigidly align three landmarks on the atlas rib with three landmarks on the subject rib. 2) Affine transformation is applied. 3) Non-rigid, non-linear transformation is applied.

Differences in the 3D models of the registered atlas rib and subject rib were compared with a deviation analysis within Geomagic Studio version 12.1.0 (Geomagic, Research Triangle Park, NC) to quantify the robustness of the image registration. The acceptable ranges of deviation were set based on the scan resolution (pixel spacing: 0.74 mm by 0.74 mm; slice thickness: 0.625 mm). Acceptable ranges corresponded to the maximum voxel length of the scan, 0.74 mm. Results are presented in Figure 7 with the color bar illustrating the deviations in millimeters between the two 3D models. Over 99% of the deviations fell within the acceptable range of -0.74 to 0.74 mm. The average deviations in the positive and negative directions were 0.194 and -0.138 mm, respectively with a standard deviation of 0.222 mm. The maximum deviations in the positive and negative directions were 1.208 and -3.109 mm, respectively. However, these deviations occurred in very localized regions on the rib and accounted for less than 1% of the overall deviations.

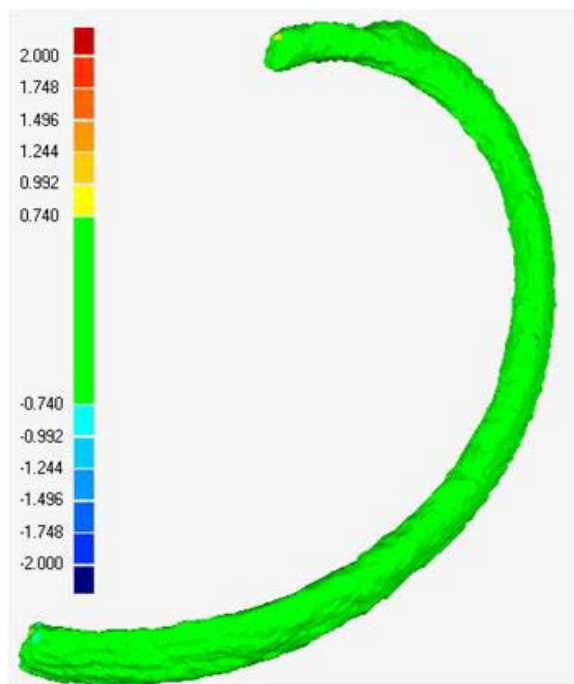


Figure 7. Deviation analysis with color bar indicating over 99% of the deviations fall in the acceptable range (± 0.74 mm).

DISCUSSION

The image segmentation and registration algorithm developed in the study provides a method for collecting extensive homologous landmark data from the ribs. The algorithm improves on the previous methods of measuring rib geometry by utilizing the full 3D information in the scan to collect landmarks

(Kent, Lee et al. 2005; Gayzik, Yu et al. 2008). The algorithm requires little user interaction, allowing landmarks to be collected in an automated fashion for a large number of subjects and reducing intra-observer and inter-observer error. Landmarks on the ribs can be classified as: true anatomical landmarks representing a homologous structure, pseudolandmarks defined by relative locations such as the most lateral point, or semilandmarks defined relative to other landmarks. Previous methods have relied on the manual landmark identification and this method may not result in selection of homologous landmarks, particularly for pseudolandmarks or semilandmarks (Gayzik, Yu et al. 2008). Automatic selection of landmarks through image registration eliminates error in landmark identification and improves the ability to select a large number of homologous landmarks on the ribs.

Limitations include the possible introduction of error since some manual interaction was required to segment the ribs. The CT scan resolution presents a limiting factor on the rib cage variation that can be detected as differences less than the maximum voxel length cannot be accurately measured. Efforts were made to select higher resolution CT scans with a slice thickness ranging from 0.625 mm to 1.25 mm to address this limitation.

Image registration has been widely used to study injuries, disease, and cancers of the brain (Maldjian, Chalela et al. 2001; Lee, Wen et al. 2010; Long and Wyatt 2010). The image segmentation and registration algorithm developed in the current study could be modified and used in subsequent research studies to collect landmark data from other bony and soft tissue anatomy. Similar to the current study, geometrical variation in the anatomy could be characterized for different ages or genders. The algorithm could also be used to study pathology and volumetrically characterize the extent and location of injured or diseased tissue.

The homologous landmark data collected with the image segmentation and registration algorithm will be input into a geometric morphometrics analysis, particularly the Procrustes superimposition method, to formulate age and gender-specific shape and size variation functions of the rib cage. Additional research will be conducted to quantify changes in bone mineral density and cortex thickness and generate functions describing variation with age and gender.

Previous studies have altered geometrical and structural characteristics of thoracic finite element

(FE) models to represent subjects of different ages (Kent, Lee et al. 2005; Ito 2009; El-Jawahri 2010). Kent et al. (2005) modified an existing FE thorax model to create three models: 1) An “up” model where the ribs were rotated upward until the ninth rib was rotated seven degrees, 2) An “old” model where the bone material properties were reduced by 30%, and 3) A “thin” model where the rib cortical shell thickness was reduced by 40% (Kent, Lee et al. 2005). Ito et al. (2009) and El-Jawahri et al. (2010) used age-specific geometry and material criteria from the literature and modified existing FE models to represent 35 year, 55 year, and 75 year old mid-size males (Ito 2009; El-Jawahri 2010).

The extensive amount of data collected in the current study will supplement existing data in the literature and more fully characterize rib morphology across ages and genders. The efficiency and efficacy of the semi-automated image segmentation and registration algorithm allows for collection of rib landmarks at a high resolution from hundreds of subjects over a wide range of ages (0-100 years) and across genders. The morphological functions developed from this landmark data will be used to create a parametric FE model of the thorax that can be scaled to represent a subject of a particular age and gender. This model will allow vehicle crashworthiness to be evaluated for all ages and genders and will lead to improvements in restraint systems to better protect children and elderly in a crash.

CONCLUSIONS

A semi-automated image segmentation and registration algorithm was developed to collect homologous rib landmarks from normal CT scans of males and females ages 0-100. The algorithm uses rigid, affine, and non-rigid, non-linear transformations to morph segmented ribs from different subjects to a rib atlas. The collected landmarks will be analyzed to formulate age and gender-specific shape and size variation functions. Results of this study will lead to an improved understanding of the complex relationship between thoracic geometry, age, gender, and injury risk.

ACKNOWLEDGEMENTS

Funding was provided by the National Highway Traffic Safety Administration and the National Science Foundation Graduate Research Fellowship Program. The authors would like to thank Dr. Leon Lenchik for providing assistance with exclusion criteria and CT scan normality. Hannah Kim, Callistus Nguyen, Hannah Reynolds, and Colby

White assisted with data collection. Dr. Chris Wyatt and Haiyong Xu provided technical assistance on the image segmentation and registration algorithm development.

REFERENCES

Allen, G. S. and N. E. Coates (1996). "Pulmonary contusion: a collective review." Am Surg **62**(11): 895-900.

Bergeron, E., A. Lavoie, et al. (2003). "Elderly Trauma Patients with Rib Fractures Are at Greater Risk of Death and Pneumonia." J Trauma **54**(3): 478-485.

Bulger, E. M. M. D., M. A. M. D. Arneson, et al. (2000). "Rib Fractures in the Elderly." Journal of Trauma-Injury Infection & Critical Care **48**(6): 1040-1047.

U.S. Census Bureau (2008). An Older and More Diverse Nation by Midcentury. P. Division, Public Information Office.

Burstein, A. H., D. T. Reilly, et al. (1976). "Aging of bone tissue: mechanical properties." J Bone Joint Surg Am **58**(1): 82-86.

Cavanaugh, J. M. (2002). Biomechanics of Thoracic Trauma. Accidental Injury: Biomechanics and Prevention. J. M. Alan M. Nahum. New York, Springer-Verlag: 374-404.

Dougall, A. M., M. E. Paul, et al. (1977). "Chest Trauma-Current Morbidity and Mortality." J Trauma **17**(7): 547-553.

El-Jawahri, R. E., Laituri, T.R., Ruan, J.S., Rouhana, S.W., Barbat, S.D. (2010). "Development and Validation of Age-Dependent FE Human Models of a Mid-Sized Male Thorax." Stapp Car Crash Journal **54**: 407-430.

Finelli, F. C., J. Jonsson, et al. (1989). "A Case Control Study for Major Trauma in Geriatric Patients." J Trauma **29**(5): 541-548.

Galan, G., J. C. Penalver, et al. (1992). "Blunt chest injuries in 1696 patients." Eur J Cardiothorac Surg **6**(6): 284-287.

Gayzik, F. S., M. M. Yu, et al. (2008). "Quantification of age-related shape change of the

human rib cage through geometric morphometrics." J Biomech **41**(7): 1545-1554.

Hanna, R., Hershman, Lawrence (2009). Evaluation of Thoracic Injuries Among Older Motor Vehicle Occupants. Washington, DC, National Highway Traffic Safety Administration.

Holcomb, J. B., N. R. McMullin, et al. (2003). "Morbidity from rib fractures increases after age 45." J Am Coll Surg **196**(4): 549-555.

Ito, O., Dokko, Y., Ohashi, K. (2009). Development of adult and elderly FE thorax skeletal models. Society of Automotive Engineers. Paper number 2009-01-0381.

Kent, R., S. H. Lee, et al. (2005). "Structural and material changes in the aging thorax and their role in crash protection for older occupants." Stapp Car Crash J **49**: 231-249.

Lee, J. W., P. Y. Wen, et al. (2010). "Morphological characteristics of brain tumors causing seizures." Arch Neurol **67**(3): 336-342.

Long, X. and C. Wyatt (2010). An Automatic Unsupervised Classification of MR Images in Alzheimer's Disease. 23rd IEEE Conference on Computer Vision and Pattern Recognition, San Francisco, USA.

Maldjian, J. A., J. Chalela, et al. (2001). "Automated CT segmentation and analysis for acute middle cerebral artery stroke." AJNR Am J Neuroradiol **22**(6): 1050-1055.

National Center for Health Statistics, N. (2003). Health, United States, 2002, Special Excerpt: Trend Tables on 65 and Older Population, Centers for Disease Control and Prevention/National Center for Health Statistics, Department of Health and Human Services.

Perdue, P. W., D. D. Watts, et al. (1998). "Differences in Mortality between Elderly and Younger Adult Trauma Patients: Geriatric Status Increases Risk of Delayed Death." J Trauma **45**(4): 805-810.

Ruan, J., R. El-Jawahri, et al. (2003). "Prediction and analysis of human thoracic impact responses and injuries in cadaver impacts using a full human body finite element model." Stapp Car Crash J **47**: 299-321.

Shorr, R. M., A. Rodriguez, et al. (1989). "Blunt Chest Trauma in the Elderly." J Trauma **29**(2): 234-237.

Stawicki, S. P., M. D. Grossman, et al. (2004). "Rib fractures in the elderly: a marker of injury severity." J Am Geriatr Soc **52**(5): 805-808.

Stitzel, J. D., P. D. Kilgo, et al. (2010). "Age thresholds for increased mortality of predominant crash induced thoracic injuries." Ann Adv Automot Med **54**: 41-50.

Zhou, Q., Rouhana, Stephen W., Melvin, John W. (1996). "Age Effects on Thoracic Injury Tolerance." Stapp Car Crash J Paper **962421**.

Zioupos, P. and J. D. Currey (1998). "Changes in the stiffness, strength, and toughness of human cortical bone with age." Bone **22**(1): 57-66.